Current Cardiology Reports (2019) 21: 60
https://doi.org/10.1007/s11886-019-1147-3

NUCLEAR CARDIOLOGY (V DILSIZIAN, SECTION EDITOR)

# The Cardiorenal Axis: Myocardial Perfusion, Metabolism, and Innervation

Jamshid Shirani[1] · Srinidhi Meera[1] · Vasken Dilsizian[2]

Published online: 20 May 2019
© Springer Science+Business Media, LLC, part of Springer Nature 2019

## Abstract

**Purpose of the Review** Cardiorenal syndrome (CRS), defined as concomitant heart and kidney disease, has been a focus of attention for nearly a decade. As more patients survive severe acute and chronic heart and kidney diseases, CRS has emerged as an "epidemic" of modern medicine. Significant advances have been made in unraveling the complex mechanisms that underlie CRS based on classification of the condition into five pathophysiologic subtypes. In types 1 and 2, acute or chronic heart disease results in renal dysfunction, while in types 3 and 4, acute or chronic kidney diseases are the inciting factors for heart disease. Type 5 CRS is defined as concomitant heart and kidney dysfunction as part of a systemic condition such as sepsis or autoimmune disease.

**Recent Findings** There are ongoing efforts to better define subtypes of CRS based on historical information, clinical manifestations, laboratory data (including biomarkers), and imaging characteristics. Systematic evaluation of CRS by advanced cardiac imaging, however, has been limited in scope and mostly focused on type 4 CRS. This is in part related to lack of clinical trials applying advanced cardiac imaging in the acute setting and exclusion of patients with significant renal disease from studies of such techniques in chronic HF.

**Summary** Advanced cardiac nuclear imaging is well poised for assessment of the pathophysiology of CRS by offering a myriad of molecular probes without the need for nephrotoxic contrast agents. In this review, we examine the current or potential future application of advanced cardiac imaging to evaluation of myocardial perfusion, metabolism, and innervation in patients with CRS.

**Keywords** Myocardial perfusion · Myocardial metabolism · Myocardial innervation · Cardiorenal syndrome · Positron emission tomography · Single photon emission computed tomography

**Abbreviations**

| | |
|---|---|
| AKI | Acute kidney injury |
| BMIPP | β-Methyl-p-[$^{123}$I]-iodophenyl-pentadecanoic acid |
| CAD | Coronary artery disease |
| CKD | Chronic kidney disease |
| CRS | Cardiorenal syndrome |
| ESRD | End-stage renal disease |
| FDG | 2-Deoxy-2-$^{18F}$fluoro-d-glucose |
| GFR | Glomerular filtration rate |
| HF | Heart failure |
| HMR | Heart-to-mediastinal ratio |
| LV | Left ventricle (ventricular) |
| mIBG | Meta-iodobenzylguanidine |
| MPI | Myocardial perfusion imaging |
| PET | Positron emission tomography |
| RAAS | Renin angiotensin aldosterone system |
| SNS | Sympathetic nervous system |
| SPECT | Single photon emission computed tomography |
| WR | Washout rate |

This article is part of the Topical Collection on *Nuclear Cardiology*

✉ Jamshid Shirani
jamshid.shirani@sluhn.org

Srinidhi Meera
Srinidhi.meera@sluhn.org

Vasken Dilsizian
VDILSIZIAN@umm.edu

[1] Department of Cardiology, St. Luke's University Health Network, Bethlehem, Ostrum Street, Bethlehem, PA 18015, USA

[2] Department of Diagnostic Radiology and Nuclear Medicine, The University of Maryland School of Medicine, Baltimore, MD 21201, USA

## Introduction

The history of modern cardiovascular medicine is marked by progressive specialization, unraveling of complex

pathophysiological processes, prevention and earlier diagnosis, as well as implementation of sophisticated and evidence-based therapeutic approaches that have collectively reduced mortality from most forms of heart disease [1]. An inevitable consequence of this dramatic success has been the emergence of an epidemic of advanced and end-stage cardiac disease in older individuals with various comorbidities and manifestations of heart disease as a systemic, rather than an organ-specific, illness [2–8]. Kidney disease is among the most common coexisting conditions in patients with acute or chronic heart disease [8]. Thus, more than half of patients with acute decompensated heart failure (HF) have some degree of renal insufficiency [9]. In addition, one in six patients identified as having stage 4 or greater chronic kidney disease (CKD) also has HF, and prevalence of HF as a diagnosis doubles in the presence of CKD [10, 11]. Coexisting HF and kidney disease is the result of complex pathophysiologic processes that present significant diagnostic, prognostic, and therapeutic challenges to the clinician [12]. The complexity of the condition is well reflected in the popularized concept of "cardiorenal syndromes (CRSs)" that currently recognizes five different pathophysiological pathways to concomitant heart and kidney disease [13]. In clinical practice, however, the boundaries of each of these scenarios are not yet sharply defined although each would likely demand and deserve its own unique diagnostic and therapeutic approach. There are ongoing efforts to define subtypes of CRS based on historical information, clinical manifestations, laboratory data (including biomarkers) [14], and imaging characteristics. Systematic evaluation of CRS by advanced cardiac imaging, however, has been limited in scope and mostly focused on type 4 CRS. This review focuses on established and potential uses of advanced cardiac imaging to assess myocardial perfusion, metabolism, and innervation in CRS.

**Cardiorenal Syndromes** CRS has been defined as "disorders of the heart and kidneys whereby acute or chronic dysfunction in one organ may induce acute or chronic dysfunction of the other" [13]. Additionally, certain systemic diseases can affect both organs. Hence, five subtypes of CRS have been identified: in types 1 and 2, acute or chronic heart disease results in renal dysfunction, while in types 3 and 4, acute or chronic kidney diseases are the inciting factors for HF. Type 5 CRS is defined as concomitant heart and kidney dysfunction as part of an acute or chronic systemic condition. Epidemiology of CRS has been recently reviewed [15•]. Accordingly, type 1 (acute cardiorenal) CRS is shown to occur in ~25% of patients hospitalized with acute decompensated HF more than half of whom have some degree of pre-existing CKD. Worsening kidney function in type 1 CRS is shown to be an independent risk factor for mortality in this setting. Type 2 (chronic cardiorenal) CRS has been more difficult to define. It is estimated that 45–63% of patients with chronic HF have evidence of CKD. Type 3 (acute renocardiac) CRS often occurs in the elderly with acute severe illness requiring intensive care. Nearly 70% of patients in such a setting have some degree of acute kidney injury (AKI) that can be severe in ~ 5–25%. Type 4 (chronic renocardiac) CRS has been shown to develop at an annualized rate of 10% in patients transitioning from stage 4 CKD to end-stage renal disease (ESRD). Type 5 (secondary) CRS may manifest acutely in conditions such as sepsis or more insidiously in systemic diseases such as autoimmune disease, sarcoidosis, or amyloidosis among others. Acute decompensated HF and acute kidney failure are associated with significantly higher mortality when accompanied by AKI or HF, respectively [16, 17•].

**Pathophysiology** The heart and the kidneys are closely linked through complex physiological processes that primarily aim at maintaining homeostasis. Tissue injury in each of the two organs, however, sets off a cascade of local and systemic responses that adversely affects the other. These responses encompass a large range of abnormalities that involve inflammatory, immune and stress-mediated reactions, neurohormonal, metabolic and nutritional mechanisms as well as changes in fluid and acid-base status, minerals, and blood viscosity. The sequence of events and timing of participation of each of these mechanisms in development of cardiac and renal abnormalities are different depending on the type of CRS.

*Type 1 and 2 CRS.* Decompensated HF is characterized by increased cardiac filling pressures and ventricular wall stress that would result in muscle fiber stretch, myocyte necrosis, and both systemic/pulmonary congestion and reduced cardiac output. These hemodynamic abnormalities subsequently lead to decreased renal arterial flow, elevated renal venous pressure, reduced glomerular filtration rate (GFR), and renal interstitial edema and hypoxia. Decreased cardiac output and venous congestion will then activate the sympathetic nervous (SNS) and renin-angiotensin aldosterone (RAAS) systems; promote release of arginine-vasopressin, endothelin, and inflammatory cytokines; and result in systemic inflammatory response and oxidative stress that in turn worsen cardiac and renal function [18•]. It is now clear that in majority of patients with decompensated HF, venous congestion plays a far more important role in pathogenesis of renal dysfunction than low cardiac output [19]. Several studies have shown a better correlation between higher right atrial pressure than lower cardiac index or ejection fraction and kidney dysfunction in HF [9, 20, 21]. Recently, a strong correlation has been demonstrated between venous Doppler patterns reflecting renal congestion and progression of HF [22]. In addition, promising techniques such as bioimpedence vector analysis are being developed and tested to allow rapid and early detection of hemodynamic alterations in patients with heart disease [23••].

HF should be considered a systemic disease that affects renal function in multiple ways regardless of left ventricular

(LV) ejection fraction. The systemic nature of HF is well evidenced by the elevated plasma levels of biomarkers of vasoconstriction, inflammation, oxidative stress, and endothelial activation in response to venous congestion, tissue hypoperfusion, and neurohormonal activation [24]. Eventually, the normal compensatory mechanisms that had aimed at maintaining hemostasis will fail, and pathologic remodeling is established [25]. At the ultrastructural level, pathologic cardiac remodeling is characterized by abnormalities of the myocyte and non-myocyte (collagen matrix, microvasculature, and cardiac innervation) compartments of the myocardium [25]. These include myocyte hypertrophy and re-expression of fetal genes, decreased contractile protein and phosphocreatine content, reduced expression of $\beta_1$-adrenergic receptors, and a metabolic switch from predominant fatty acid to glucose utilization [26]. In addition, continued pathologic loading conditions ultimately leads to myocyte cell loss through necrotic, apoptotic, and autophagic pathways [27]. Coronary artery disease, reduced capillary density, pathologic fibrosis, and expanded collagen matrix further accentuate pathologic cardiac remodeling [28]. Systemic and local activation of the SNS and RAAS is also a major contributor to the myocardial ultrastructural changes in HF [29, 30]. Kidney dysfunction in advanced HF is the result of hemodynamic abnormalities (decreased cardiac output, elevated right-sided filling pressures, and hypotension) as well as neurohormonal, activation, systemic inflammatory/immune response, and oxidative stress. A clinical dilemma in evaluation of kidney dysfunction in patients with chronic HF is whether or not concomitant kidney dysfunction is a consequence of the heart disease or an independent entity [31]. In most cases, clinical and laboratory data allows such a distinction, but significant overlap still exists [32].

*Type 3 CRS.* Significant recent advances have been made in discovery of biomarkers of acute kidney injury including those specific to ischemic, immune-mediated, or nephrotoxic damage [33••]. Biomarkers such as B-type natriuretic peptide and its prohormone, cardiac troponins, and heart-fatty acid-binding protein have also been helpful in diagnosis of HF in patients with acute kidney injury [33••]. Elevations in plasma level of such biomarkers are the results of both the systemic (direct) and the hemodynamic (indirect) components of renal injury and their effects on cardiovascular function [34].

*Type 4 CRS.* Anatomically and as assessed by renal ultrasound, the kidney in CKD and ESRD often appears smaller than normal with loss of fine structure and with subcortical and medullary cysts as well as calcific deposits [35]. Studies of type 4 CRS have predominantly focused on HF in patients with CKD and ESRD. However, similar to HF, advanced kidney disease should be considered a systemic disease with both hemodynamic and non-hemodynamic components that affect the heart as well as other organs [36]. A large necropsy study of patients on chronic hemodialysis has shown a wide range of structural cardiovascular abnormalities including left and right ventricular hypertrophy and dilation as well as calcific deposits in the coronary arteries, aortic valve, mitral annulus, and thoracoabdomianl aorta [37]. Obstructive coronary artery disease (CAD) [39%] and severe aortic stenosis (8%) were also present, and over 50% of patients with known causes of death died of cardiovascular events [37]. Clinical counterpart of these pathologic findings has been the high prevalence of CAD, HF, valvular heart disease, and pulmonary hypertension in patients with CKD and ESRD [38]. In addition, studies using non-contrast (native) magnetic resonance T1 mapping have demonstrated myocardial fibrosis as a precursor to further LV remodeling and reduced LV mechanics [39]. The increased myocardial fibrosis in CKD is likely multifactorial and represents the interplay of LV pressure and volume overload, comorbid conditions and blood supply, and demand mismatch.

*Type 5 CRS.* This type CRS encompasses a wide range of systemic conditions that simultaneously or sequentially affect cardiac and renal function. These conditions may have an acute (sepsis, drugs, toxins) or insidious (connective tissue disorders, sarcoidosis) onset of effect on the two organs. Although the end result of these processes may appear similar, with reference to cardiac and renal injury, each of these conditions has its unique pathophysiologic features [40].

**Cardiac Imaging in CRS** In types 1–3 CRS, the presence of renal or cardiac impairment enhances underlying functional and anatomic abnormalities of the other organ through hemodynamic, neurohormonal activation and other systemic mediators. These abnormalities are reflected in alterations in myocardial perfusion, metabolism, and innervation among others. Chronic and end-stage renal disease adds a new dimension to these abnormalities through additional abnormalities in lipid metabolism, calcium hemostasis, existing coronary artery disease, hypertension, diabetes, anemia, the effects of arteriovenous shunts used for chronic hemodialysis, and the cardiotoxicitiy of uremic toxins [41]. It should be noted that data specific to each of these physiologic abnormalities relevant to particular type of CRS is scarce and differential impact of renal dysfunction on cardiac perfusion, metabolism, or innervation has not been fully investigated.

**Myocardial Perfusion** The presence of renal dysfunction often limits the use of radiographic and magnetic resonance contrast agents due to concerns regarding contrast-induced nephropathy and nephrogenic systemic sclerosis. Consequently, routine invasive angiography, coronary computed tomographic angiography, and cardiac magnetic resonance with gadolinium-based contrast agents have limited use in this setting. In addition, in the case of chronic CKD, coronary calcium scoring with computed tomography is of limited diagnostic or prognostic value due to the presence of extensive and premature

(often medial) calcification disproportionate to the severity of obstructive CAD [42–45]. Regional myocardial perfusion in this setting is, thus, frequently assessed with the use of single photon emission computed tomography (SPECT) or positron emission tomography (PET) [46–52]. Extensive experience exists regarding diagnostic and prognostic performance of SPECT myocardial perfusion imaging (MPI) in patients with HF, CKD, or both [47]. In general, both diagnostic and prognostic accuracy of SPECT is reduced as the duration and severity of CKD increases. The most important limitation of SPECT MPI is in its reliance on myocardial segments with "normal" perfusion to be used as a reference for determining relative hypoperfusion in abnormal regions [51]. Unfortunately, heterogeneity in myocardial perfusion is frequently observed in pressure and volume-overloaded human hearts. Other limitations of SPECT MPI are related to the performance of the clinically available SPECT MPI studies in relation to relatively low extraction fraction of $^{99m}$Technetium (Tc)-based tracers, clinical setting (inability to exercise, abnormal electrocardiogram, diffuse CAD with "balanced" reduction in coronary flow reserve), and lack of adequate response to vasodilator stressors in those with endothelial dysfunction or marked coronary medial calcification. Consequently, a normal SPECT MPI study may not necessarily indicate a low short-term cardiac event rate in patients with ESRD [53], and false-positive studies are not uncommon. Many of these limitations are effectively avoided with quantification of global and regional myocardial blood flow with PET particularly in relation to detection of multivessel CAD that may present with a balanced reduction of myocardial blood flow [48–52]. Simultaneous assessment of myocardial perfusion and coronary flow reserve by PET MPI may also have the advantage of identifying patients with CKD and diffuse "non-obstructive" coronary atherosclerosis, microvascular disease, or abnormally elevated resting myocardial blood flow [54••, 55]. Among PET perfusion tracers, $^{13}$N-ammonia and $^{82}$Rb-rubidium are approved for clinical use, and $^{15}$O-water is used in research laboratories. $^{82}$Rb-rubidium can now be produced locally by a closed system generator that obviates the need for a cyclotron [56]. A new, $^{18}$F-labeled tracer ($^{18}$F-flurpiridaz) is undergoing phase III clinical trials and has many advantages over the current tracers including longer half-life (~ 110 min), higher spatial resolution, and greater myocardial extraction fraction [57]. It binds specifically and reversibly to the complex 1 (NADH/ubiquinone oxidoreductase), the enzymatic system located in the inner mitochondrial membrane and involved in synthesis of adenosine triphosphate (Fig. 1).

**Myocardial Metabolism** Metabolic abnormalities and alterations in substrate utilization have been long recognized in the failing hearts of patients with ischemic and non-ischemic cardiomyopathies. Early adaptive changes include a shift from predominantly fatty acid oxidation (aerobic) to glucose (anaerobic) metabolism aimed at maintaining cell survival through balancing oxygen consumption and energy production [58]. Such metabolic adaptation occurs by upregulation of glucose uptake and downregulation of fatty acid oxidation that collectively allow energy production at substantially reduced cost. Several molecular metabolic probes have been used to assess myocardial substrate utilization in clinical practice [59–65]). The PET tracer, 2-deoxy-2-$^{18F}$fluoro-d-glucose (FDG), is the most commonly used probe for evaluation of myocardial glucose metabolism. FDG is a glucose analog that is phosphorylated by hexokinase to FDG-6-phosphate and is retained intracellularly without further metabolism. When combined with perfusion imaging, FDG PET allows reliable detection of viable myocardium in ischemic cardiomyopathy [65]. Hibernating myocardium is characterized by perfusion-metabolism mismatch where metabolic activity is observed in areas with reduced perfusion [59, 63, 64••]. Applying quantitative analysis of FDG PET images, it has been shown that myocardial glucose utilization is inversely correlated to estimated GFR in non-diabetic adults with CKD irrespective of age, gender, race, or myocardial workload [66••] (Fig. 2). The latter can be explained by the observation that myocardial ischemia in the absence of epicardial CAD is commonly observed in patients with CKD due to structural and functional abnormalities that include LV hypertrophy, interstitial fibrosis, and decreased myocardial capillary density [67]. Energy starvation, recurrent global ischemia, and metabolic remodeling can, thus, occur in the hearts of patients with CKD in parallel to severity of renal dysfunction.

Repetitive myocardial stunning has been also observed during hemodialysis. In a small (four patients, three diabetic) study of myocardial blood flow during dialysis, $^{15}$O-water PET imaging demonstrated acute reduction in myocardial blood flow associated with appearance of transient regional LV wall motion abnormality on echocardiography [68]. In another study of seven non-diabetic adults, the reduction in myocardial blood flow during hemodialysis, as assessed by $^{13}$N-ammonia PET, occurred relatively early during the procedure such that the ensued myocardial ischemia could not be fully explained on the basis of hypovolemia alone [69]. Severe intradialytic myocardial stunning is shown to occur more commonly in men with more severe LV hypertrophy and systolic dysfunction [70] and has been associated with elevated serum troponin levels [71] and higher mortality [72]. Although the pathophysiology of myocardial stunning during

**Fig. 1** Representative examples of normal (**a**) and abnormal (**b**) $^{18}$F-flurpiridaz PET myocardial perfusion images are shown. In **a**, consecutive tomograms of paired stress (upper row) and rest (lower row) images show normal distribution of the radiotracer in all myocardial regions. In **b**, paired stress and rest images show extensive reversible regional perfusion defects in all three three coronary artery vascular territories associated with transient ischemic cavity dilatation. (Reproduced with permission from: Dilsizian V, Taillefer R. *JACC Cardiovasc Imaging* 2012;5:1269–1284) [57]

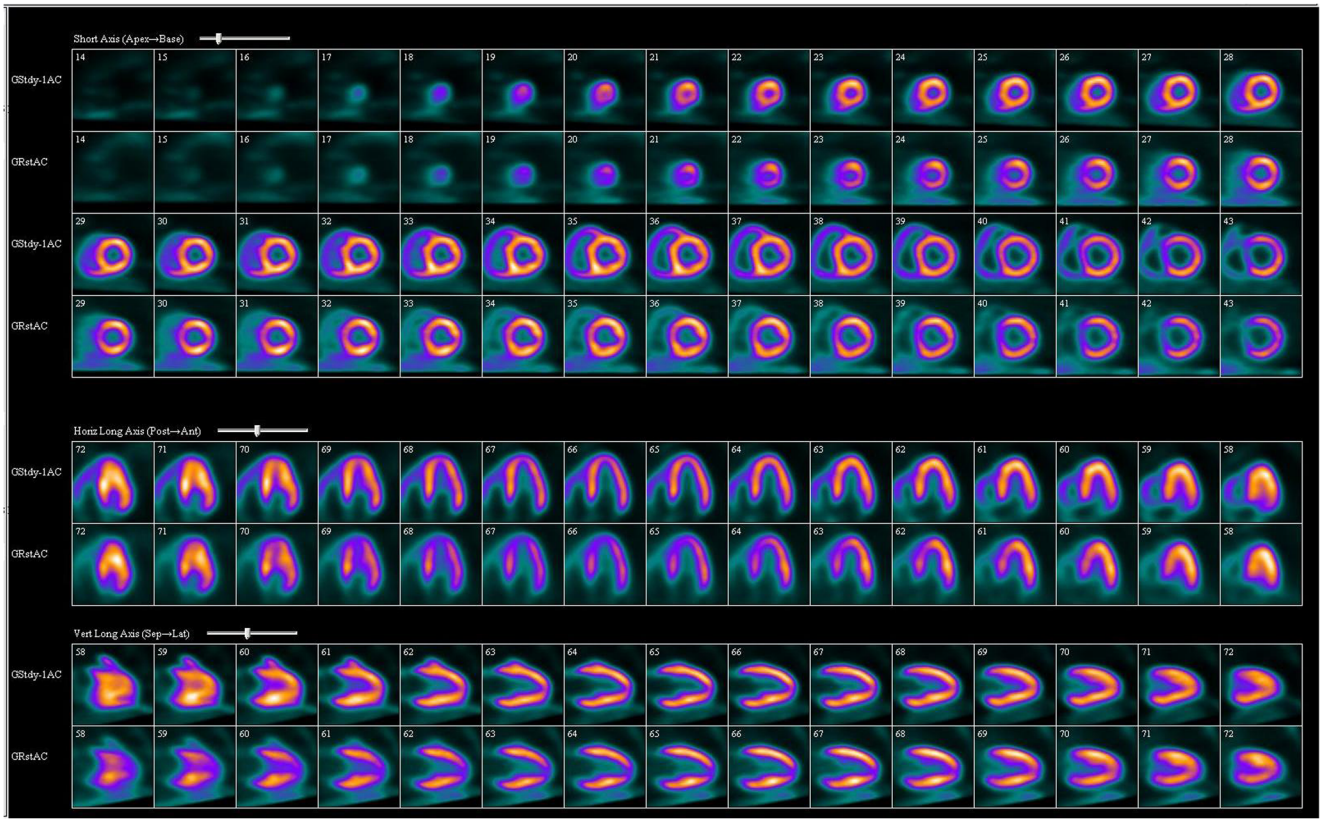
Short Axis (Apex→Base)
GStdy-1AC
GRstAC
Horiz Long Axis (Post→Ant)
Vert Long Axis (Sep→Lat)

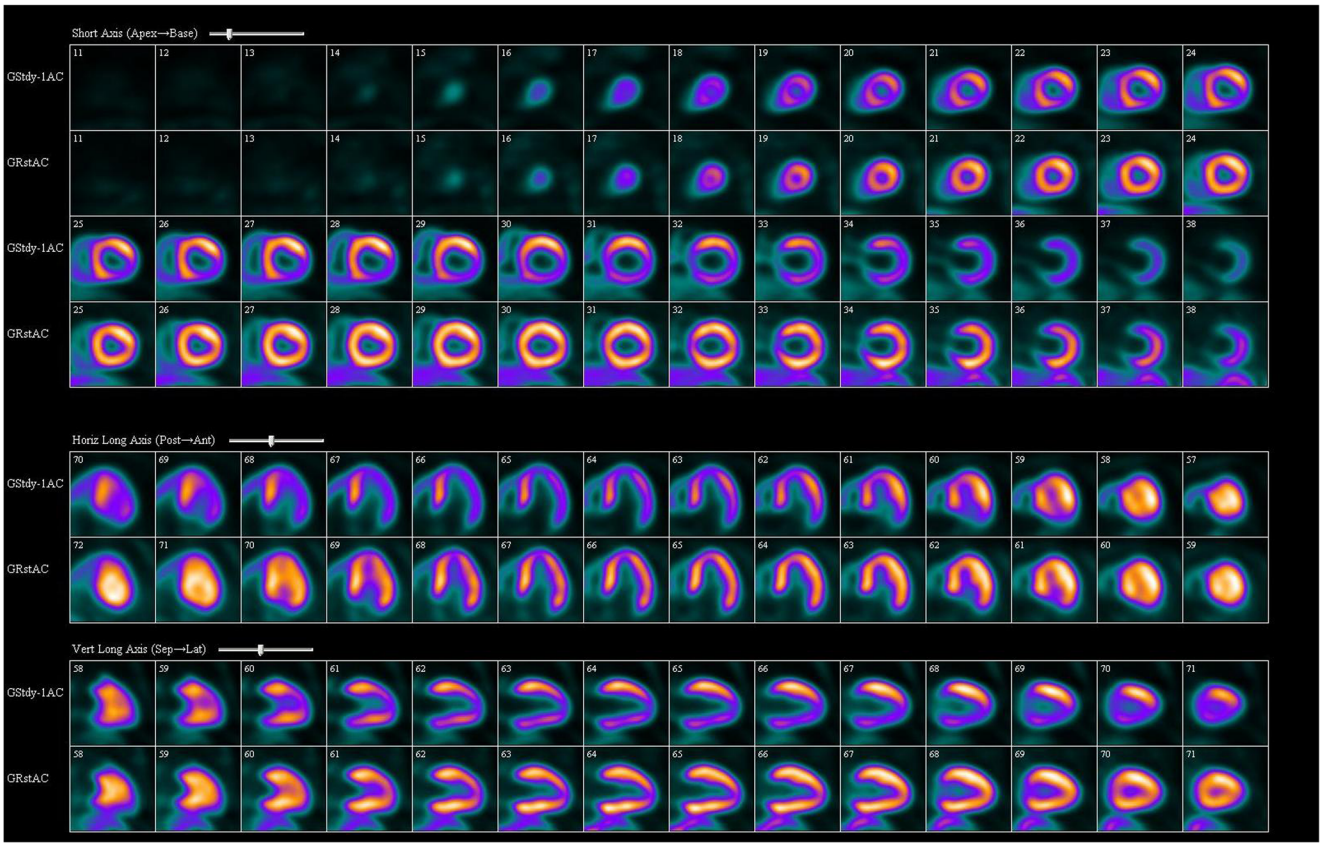
Short Axis (Apex→Base)
GStdy-1AC
GRstAC
Horiz Long Axis (Post→Ant)
Vert Long Axis (Sep→Lat)

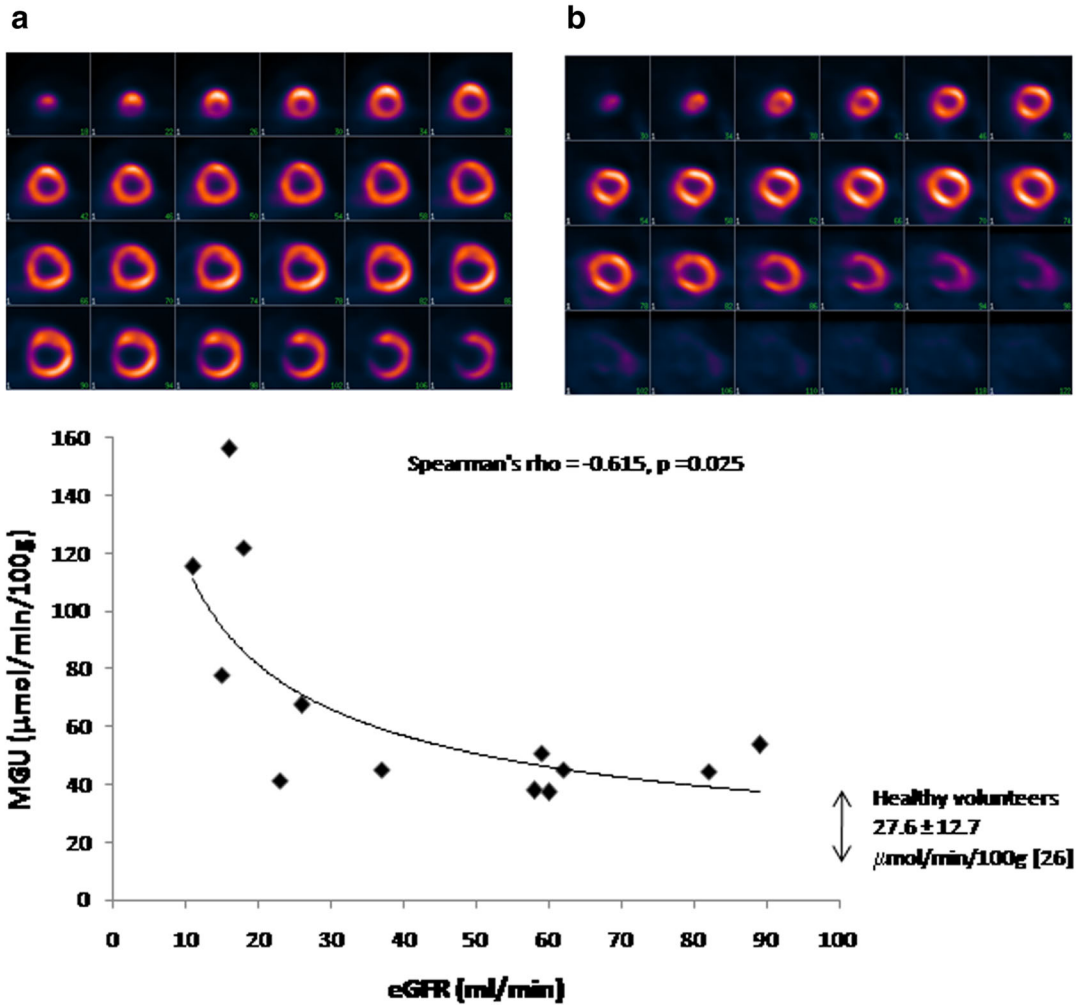


**Fig. 2** Examples of myocardial FDG distribution in CKD patients exhibiting no visually discernable regional defects. **a** A representative example of a CKD patient with dilated left ventricular cavity and concentric hypertrophy. **b** A CKD patient with normal left ventricular cavity size without hypertrophy. **c** Scatter plot of estimated glomerular filtration rate (ml/min/1.73 $m^2$) versus myocardial glucose uptake (μmol/min/100 g) as measured by 18F-fluorodeoxyglucose PET scan in CKD. The *fitted line* is MGU = $k$ × eGFRx with estimated fitting parameters $k = 385.2$ ($p < 0.00001$) and $x = -0.520$ ($p = 0.002$). (Reproduced with permission from S. Karger AG, Basel from: Fink JC, et al. *Cardiology* 2010;116:160–167) [66]

dialysis is not fully elucidated, it is likely that autonomic dysregulation and abnormal myocardial sympathetic innervation in ESRD play significant roles in its pathogenesis.

In addition to glucose metabolism, myocardial fatty acid oxidation can be evaluated by several molecular probes including β-methyl-p-[$^{123}$I]-iodophenyl-pentadecanoic acid (BMIPP). BMIPP is a radioiodine-labeled branched-chain fatty acid that is taken up by the myocyte and is trapped within the lipid pool after initial adenosine triphosphate-dependent thioesterification and no further significant mitochondrial β-oxidation. BMIPP SPECT imaging has been found to be useful in detection of regionally reduced myocardial fatty acid metabolism up to 30 h after an episode of transient myocardial ischemia (termed "ischemic memory") [73–75]. Such a relationship between myocardial ischemia and metabolism is also noted and may be accentuated in patients with CKD [76] (Fig. 3). When applied to patients with ESRD, BMIPP-rest thallium dual-isotope SPECT was highly accurate in identifying CAD defined as ≥ 75% coronary artery luminal narrowing by invasive angiography [77]. It was then shown that decreased myocardial fatty acid metabolism, as assessed by BMIPP SPECT, is associated with insulin resistance and impaired LV systolic function in diabetic and non-diabetic ESRD patients without CAD [78]. In addition, severely abnormal BMIPP SPECT has been predictive of acute myocardial infarction, heart failure, and cardiac (including sudden) death in ESRD [79]. The prognostic value of abnormal BMIPP SPECT in hemodialysis patients has been extended to those undergoing percutaneous coronary revascularization [80]. In a multicenter trial of BMIPP SPECT in 677 asymptomatic patients on hemodialysis, cardiac death correlated directly to the severity of impaired myocardial fatty acid metabolism [81]. A

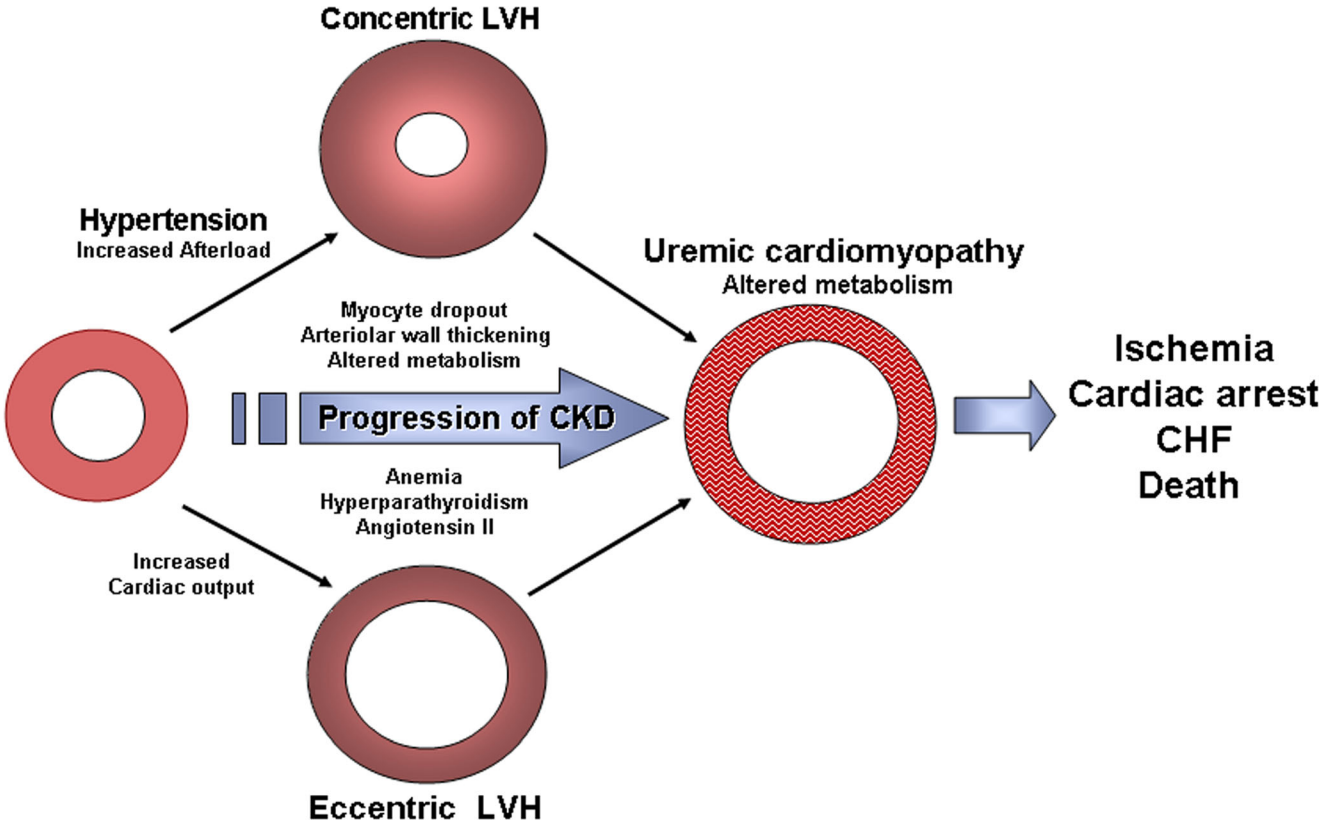


**Fig. 3** The concurrent pathogenic factors contributing to the development of uremic cardiomyopathy and altered metabolism with declining kidney function in CKD (Reproduced with permission from: Dilsizian V, Fink JC. *J Am Coll Cardiol* 2008;51:146–148) [76]

focal pattern of BMIPP defect in the left anterior descending coronary artery territory has been found to be predictive of particularly high cardiac death rate in patients on hemodialysis compared with a non-focal pattern [82]. It is likely that the high cardiac death rates among patients with ESRD and metabolic shift from fatty acid to glucose are at least partly related to ineffective glucose metabolism following transient silent ischemia. It has been known that impaired fatty acid oxidation leads to accumulation of acyl CoA that in turn disrupts glucose uptake and metabolism and ATP synthesis. Chronic myocardial energy starvation and inefficient metabolic adaptation may account for the excessive cardiovascular morbidity and mortality observed in CKD. Such metabolic inefficiency in the face of recurrent ischemia may result in myocyte cell loss and myocardial instability leading to progressive heart failure and ventricular rhythm abnormalities. Quantitative studies of simultaneous myocardial glucose and fatty acid metabolism as well as perfusion are sorely needed for further understanding of the pathophysiology of myocardial energy production and utilization in various stages of renal disease. The latter can be facilitated with the use of the many molecular probes available for the assessment of various steps of myocardial metabolism by PET imaging. Some of these promising PET tracers include labeled glucose (glucose uptake and metabolism), palmitate (fatty acid fatty acid uptake, β-oxidation, and storage as triglycerides), acetate (oxidative metabolism), and $^{15}$O-water (oxygen consumption).

**Cardiac Autonomic Innervation** Both HF and CKD present continued pathologic loading conditions that promote activation of the neurohormonal system including the SNS [83]. Neurohormonal activation at first aims to maintain homeostasis through chronotropic, inotropic, dromotropic, vasoconstrictive, and venoconstrictive effects on the heart and circulation. However, prolonged SNS stimulation (and loss of sympathetic-parasympathetic interaction) will eventually lead to adverse cardiac remodeling [84, 85]. Cardiac sympathetic innervation can be effectively assessed with the radiolabeled false neurotransmitter and norepinephrine analog $^{123}$I-metaiodobenzylguanidine ($^{123}$I-mIBG) [86••, 87]. Similar to norepinephrine, $^{123}$I-mIBG enters the sympathetic synaptic spaces and is actively taken up into and accumulates in the presynaptic adrenergic terminals by norepinephrine transporter membrane protein without interacting with postsynaptic receptors. In HF, decreased neuronal uptake of $^{123}$I-mIBG due to post-transcriptional downregulation of the cardiac norepinephrine transporter leads to accumulation of the tracer in the synaptic clefts. Reduced $^{123}$I-mIBG uptake is a strong indicator of cardiac sympathetic denervation and heightened risk of HF progression, ventricular arrhythmias, and cardiac

death [86••]. $^{123}$I-mIBG results also allow risk stratification and monitoring of the effects of various anti-remodeling therapies in HF [88•, 89•, 90•, 91•, 92•, 93•, 94•, 95•]. Evaluation of cardiac sympathetic innervation using $^{123}$I-mIBG involves semi-quantitative assessment of both planar and SPECT images. The planar images are used to assess early (15–30 min) and late (3–4 h) heart-to-mediastinal uptake ratios (HMR) by dividing the mean counts per pixel from a cardiac region of interest by the mean counts per pixel from an upper mediastinal region of interest [96]. Early HMR reflects the integrity of the presynaptic nerve terminals and uptake-1 function, while late HMR is more suggestive of the overall neuronal function including uptake, storage, and release [96]. The washout rate (WR) of the tracer, defined as the difference between early and late HMR expressed as a percentage of early HMR, predominantly reflects neuronal integrity of the adrenergic drive. An increased WR is, thus, indicative of decreased neuronal uptake of norepinephrine. SPECT images are generally used to determine the uniformity and regional distribution of myocardial $^{123}$I-mIBG often in comparison to perfusion imaging.

Elevated plasma catecholamines (dopamine and norepinephrine) is commonly observed in patients with CKD and has been shown to correlate with the WR and heterogeneity of myocardial uptake of $^{123}$I-mIBG as well as abnormal heart rate variability [97, 98]. There is evidence that in ESRD, cardiac autonomic denervation as assessed by $^{123}$I-mIBG occurs relatively early, precedes clinical myocardial ischemia or heart failure, and is directly proportional to the duration of renal disease and presence of ventricular late potentials [99, 100]. In patients with heart failure, abnormal cardiac autonomic function has been shown in some studies to be a more powerful predictor of mortality than GFR alone [101, 102]. In another study, such an abnormality was found to be synergistic with low GFR in prediction of adverse outcome [103]. In the latter study, late HMR (< 1.57) on $^{123}$I-mIBG as assessed in 468 patients with HF and reduced ejection fraction (< 50%) was highly predictive of mortality over a follow-up period of 5 years [103]. Other significant independent predictors of death were the New York Heart Association functional class, hemoglobin (< 11.9 g/dL), and estimated GFR (< 46.4 mL/min/1.73 m$^2$). When these independent predictors were combined, the collective prognostic power of the four predictors exceeded that of any individual predictor [103]). In a preliminary report of a study of 280 patients with CRS (mean age 61 years, 73% men, 26% CAD, LV ejection fraction < 50%, CKD no ESRD), late HMR of < 1.57 on $^{123}$I-mIBG scan was highly predictive of mortality (hazard ratio 6.98; 95% confidence interval 3.33–16.52; $p < 0.01$) over a mean follow-up period of 50 months [104]. Another predictor of mortality in this study was a 1 mg/dl decrease in hemoglobin level (hazard ration 1.29; 95% confidence interval 1.08–1.53; $p < 0.01$). Current use of RAAS inhibitors and beta-blockers was associated with better prognosis in CRS patients with reduced late HMR in this study [104]). Of interest, CRS alone was not a predictor of mortality (hazard ratio 1.57; 95% confidence interval 0.81–3.25; $p = 0.18$) in this study, and prognosis of CRS patients with late HMR of ≥ 1.57 was comparable with that of the non-CRS control patients [104]. The findings again emphasize the central role of cardiac autonomic denervation in adverse cardiac outcomes in patients with CKD. To date, the study of cardiac autonomic innervation in CRS remains limited to $^{123}$I-mIBG imaging. Other tracers, particularly those used in conjunction with PET imaging, can improve the understanding of this complex system. The PET tracer, $^{11}$C-meta-hydroxyephedrine, has been compared with $^{123}$I-mIBG and shown to provide better assessment of regional myocardial presynaptic sympathetic innervation [105, 106]. Comprehensive study of cardiac autonomic innervation in CRS should eventually include evaluation of beta-adrenergic, muscarinic, and nicotinic receptors as well.

**Cardiac Imaging in CRS Type 5** Type 5 CRS is characterized by simultaneous involvement of the heart and kidneys in an acute systemic disorder. This type CRS, thus, encompasses a wide range of conditions with variable pathophysiologic mechanisms and multitude of contributing factors. Tremendous advances have been made in early diagnosis, assessment of cardiac and renal involvement, and prognostication of type 5 CRS. For example, in cardiac amyloidosis, imaging with bone avid tracer, $^{99m}$Tc-pyrophosphate, has been found highly sensitive and specific in diagnosis of transthyretin cardiomyopathy and its differentiation from amyloid light chain and non-amyloid cardiomyopathy [107–109]. Disadvantage of $^{99m}$Tc-pyrophosphate is the lack of accurate quantification of cardiac amyloid burden and binding to type A (fragmented and full length) and not to type B (only full length) transthyretin fibers. These limitations has been overcome by development of a PET tracer $^{11}$C-Pittsburgh compound B that is capable of identifying both type A and B transthyretin as well as light chain amyloid deposits in the heart [110]. $^{18}$F-labeled PET tracers (florbetapir, florbetaben, and sodium floride) are in early clinical evaluation with promising preliminary reports of high sensitivity for detecting amyloid fiber deposition in the heart. A common transthyretin mutation (Val30Met) is shown to present with early cardiac sympathetic denervation as assessed by $^{123}$I-mIBG [111]. A late HMR of < 1.6 in patients with this type mutation has been shown to be associated with increased mortality [112]. In cardiac sarcoidosis, a combination of perfusion and FDG (inflammation) imaging with PET provides an excellent tool to diagnose early and late disease, identify extracardiac sites of involvement, and monitor effects of treatment [113, 114]). Coronary microvascular disease is a cardinal feature of Fabry disease and is responsible for myocardial ischemia, angina symptoms, and myocardial fibrosis and infarction in the absence of epicardial CAD. Coronary flow reserve is shown to be markedly impaired in Fabry disease, as assessed by dipyridamole $^{13}$N-ammonia PET, irrespective of LV hypertrophy and gender [115].

## Conclusions

Significant advances have been in defining the pathophysiology, clinical course, response to therapy, and prognosis of CRS. Advanced cardiac imaging has played a pivotal role in unraveling abnormalities in myocardial perfusion, metabolism, and innervation in patients with simultaneous heart and kidney disease. Data specific to each of the physiologic abnormalities relevant to particular type of CRS is, however, scarce, and differential impact of renal dysfunction on cardiac perfusion, metabolism, or innervation requires further systematic investigation.

### Compliance with Ethical Standards

**Conflict of Interest** The authors declare that they have no conflict of interest.

**Human and Animal Rights and Informed Consent** This article does not contain any studies with human or animal subjects performed by any of the authors.

## References

Papers of particular interest, published recently, have been highlighted as:
- • Of importance
- •• Of major importance


1. Mensah GA, Wei GS, Sorlie PD, Fine LJ, Rosenberg Y, Kaufmann PG, et al. Decline in cardiovascular mortality: possible causes and implications. Circ Res. 2017;120:366–80.
2. Dunlay SM, Roger VL. Understanding the epidemic of heart failure: past, present, and future. Curr Heart Fail Rep. 2014;11:404–15.
3. Mentz RJ, Kelly JP, von Lueder TG, Voors AA, Lam CS, Cowie MR, et al. Noncardiac comorbidities in heart failure with reduced versus preserved ejection fraction. J Am Coll Cardiol. 2014;64:2281–93.
4. Tsao CW, Lyass A, Enserro D, Larson MG, Ho JE, Kizer JR, et al. Temporal trends in the incidence of and mortality associated with heart failure with preserved and reduced ejection fraction. JACC Heart Fail. 2018;6:678–85.
5. Conrad N, Judge A, Tran J, Mohseni H, Hedgecott D, Crespillo AP, et al. Temporal trends and patterns in heart failure incidence: a population-based study of 4 million individuals. Lancet. 2018;391:572–80.
6. Sharma A, Zhao X, Hammill BG, Hernandez AF, Fonarow GC, Felker GM, et al. Trends in noncardiovascular comorbidities among patients hospitalized for heart failure: insights from the Get With The Guidelines-Heart Failure Registry. Circ Heart Fail. 2018;11:e004646.
7. Juillière Y, Venner C, Filippetti L, Popovic B, Huttin O, Selton-Suty C. Heart failure with preserved ejection fraction: a systemic disease linked to multiple comorbidities, targeting new therapeutic options. Arch Cardiovasc Dis. 2018: **in press**;111:766–81.
8. Conrad N, Judge A, Tran J, Mohseni H, Hedgecott D, Perez Crespillo A, et al. Temporal trends and patterns in heart failure incidence: a population-based study of 4 million individuals. Lancet. 2018;391:572–80.
9. Heywood JT, Fonarow GC, Costanzo MR, Mathur VS, Wigneswaran JR, Wynne J. High prevalence of renal dysfunction and its impact on outcome in 118,465 patients hospitalized with acute decompensated heart failure: a report from the ADHERE database. J Card Fail. 2007;13:422–30.
10. Stevens LA, Li S, Wang C, Huang C, Becker BN, Bomback AS, et al. Prevalence of CKD and comorbid illness in elderly patients in the United States: results from the Kidney Early Evaluation Program (KEEP). Am J Kidney Dis. 2010;55(suppl 2):S23–33.
11. Collins AJ, Foley RN, Chavers B, Gilbertson D, Herzog C, Ishani A, et al. US Renal Data System 2013 annual data report. Am J Kidney Dis. 2014;63(suppl 1):e1–e420.
12. House AA. Management of heart failure in advancing CKD: Core Curriculum 2018. Am J Kidney Dis. 2018;72:284–95.
13. House AA, Anand I, Bellomo R, Cruz D, Bobek I, Anker SD, et al. Definition and classification of cardio-renal syndromes: workgroup statements from the 7th ADQI Consensus Conference. *Nephrol Dial Transplant*. 2010;25:1416–20.
14. Brisco MA, Testani JM. Novel renal biomarkers to assess cardiorenal syndrome. Curr Heart Fail Rep. 2014;11:485–99.
15. • Roncoa C, Di Lullob L. Cardiorenal Syndrome in western countries: epidemiology, diagnosis and management approaches. Kidney Dis (Basel). 2017;2:151–63 **This is a comprehensive review of cardiorenal syndrome with examples of each type, epidemiology of the condition and discussion of diagnosis and management.**
16. Fonarow GC, Adams KF Jr, Abraham WT, Yancy CW, Boscardin WJ, ADHERE Scientific Advisory Committee, Study Group, and Investigators. Risk stratification for in-hospital mortality in acutely decompensated heart failure: classification and regression tree analysis. JAMA 2005;293:572–580.
17. • Mavrakanas TA, Khattak A, Singh K, Charytan DM. Epidemiology and natural history of the cardiorenal syndromes in a cohort with echocardiography. Clin J Am Soc Nephrol. 2017;12:1624–33 **This is a retrospective cohort study of adults who underwent transthoracic echocardiography between 2004 and 2014 used to derive the prevalence and natural history of various types of cardiorenal syndrome.**
18. • Harjola VP, Mullens W, Banaszewski M, Bauersachs J, Brunner-La Rocca HP, Chioncel O, et al. Organ dysfunction, injury and failure in acute heart failure: from pathophysiology to diagnosis and management. A review on behalf of the acute heart failure Committee of the Heart Failure Association (HFA) of the European Society of Cardiology (ESC). Eur J Heart Fail. 2017;19:821–36 **This is an authoritative and informative review of the current understanding of the presentation and management of concurrent organ impairment, including kidney dysfunction, in acute heart failure.**
19. Gnanaraj J, von Haehling S, Anker SD, Raj DS, Radhakrishnan J. The relevance of congestion in the cardio-renal syndrome. Kidney Int. 2013;83:384–91.
20. Nohria A, Hasselblad V, Stebbins A, Pauly DF, Fonarow GC, Shah M, et al. Cardio-renal interactions: insights from the ESCAPE trial. J Am Coll Cardiol. 2008;51:1268–74.
21. Damman K, van Deursen VM, Navis G, Voors AA, van Veldhuisen DJ, Hillege HL. Increased central venous pressure is associated with impaired renal function and mortality in a broad spectrum of patients with cardiovascular disease. J Am Coll Cardiol. 2009;53:582–8.
22. Anand IS, Greenberg BH, Katra RP, Fogoros RN, Libbus I, Katra RP, et al. Design of the Multi-Sensor Monitoring in Congestive HF (MUSIC) study: prospective trial to assess the utility of continuous wireless physiologic monitoring in heart failure. J Card Fail. 2011;17:11–6.

23.•• Puzzovivo A, Monitillo F, Guida P, Leone M, Rizzo C, Grande D, et al. Renal venous pattern: a new parameter for predicting prognosis in heart failure outpatients. J Cardiovasc Dev Dis. 2018;5: E52 **This is an insightful study that demonstrates the significance of renal congestion in predicting progression of heart failure and characterization of cardiorenal syndrome through the eyes of renal vein Doppler pattern.**

24. Cruz DN, Fard A, Clementi A, Ronco C, Maisel A. Role of biomarkers in the diagnosis and management of cardio-renal syndromes. Semin Nephrol. 2012;32:79–92.

25. Shirani J, Singh A, Agrawal S, Dilsizian V. Cardiac molecular imaging to track left ventricular remodeling in heart failure. J Nucl Cardiol. 2017;24:574–90.

26. Shirani J, Narula J, Eckelman WC, Narula N, Dilsizian V. Early imaging in heart failure: exploring novel molecular targets. J Nucl Cardiol. 2007;14:100–10.

27. Konstantinidis K, Whelan RS, Kitsis RN. Mechanisms of cell death in heart disease. Arterioscler Thromb Vasc Biol. 2012;32: 1552–62.

28. Mohammed SF, Hussain S, Mirzoyev SA, Edwards WD, Maleszewski JJ, Redfield MM. Coronary microvascular rarefaction and myocardial fibrosis in heart failure with preserved ejection fraction. Circulation. 2015;131:550–9.

29. Zhang DY, Anderson AS. The sympathetic nervous system and heart failure. Cardiol Clin. 2014;32:33–45.

30. Sayer G, Bhat G. The renin-angiotensin-aldosterone system and heart failure. Cardiol Clin. 2014;32:21–32.

31. McCullough PA, Kellum JA, Mehta RL, Murray PT, Ronco C. ADQI consensus on AKI biomarkers and cardiorenal syndromes. Contrib Nephrol. 2013;182:82–98.

32. Preeti J, Alexandre M, Pupalan I, Merlin TC, Claudio R. Chronic heart failure and comorbid renal dysfunction—a focus on type 2 cardiorenal syndrome. Curr Cardiol Rev. 2016;12:186–94.

33.•• Fu S, Zhao S, Ye P, Luo L. Biomarkers in cardiorenal syndromes. Biomed Res Int. 2018:9617363 **This is a comprehensive review of established and possibly useful biomarkers that are predictive of heart failure and renal diseases with a potential for identifying cardiac dysfunction in renal diseases and renal injury in heart failure.**

34. Clementi A, Virzì GM, Brocca A, de Cal M, Pastori S, Clementi M, et al. Advances in the pathogenesis of cardiorenal syndrome type 3. Oxidative Med Cell Longev. 2015;2015:148082.

35. Petrucci I, Clementi A, Sessa C, Torrisi I, Meola M. Ultrasound and color Doppler applications in chronic kidney disease. J Nephrol. 2018;31:863–79.

36. Zoccali C, Vanholder R, Massy ZA, Ortiz A, Sarafidis P, Dekker FW, Fliser D, Fouque D, Heine GH, Jager KJ, Kanbay M, Mallamaci F, Parati G, Rossignol P, Wiecek A, London G; European Renal and Cardiovascular Medicine (EURECA-m) Working Group of the European Renal Association - European Dialysis Transplantation Association (ERA-EDTA). The systemic nature of CKD. Nat Rev Nephrol 2017;13:344–358.

37. Roberts WC, Taylor MA, Shirani J. Cardiac findings at necropsy in patients with chronic kidney disease maintained on chronic hemodialysis. Medicine (Baltimore). 2012;91:165–78.

38. Bhatti NK, Karimi GK, Paz Y, Nazif T, Moses JW, Leon MB, et al. Diagnosis and management of cardiovascular disease in advanced and end-stage renal disease. J Am Heart Assoc. 2016;5:e003648.

39. Stromp TA, Spear TJ, Holtkamp RM, Andres KN, Kaine JC, Alghuraibawi WH, et al. Quantitative gadolinium-free cardiac fibrosis imaging in end stage renal disease patients reveals a longitudinal correlation with structural and functional decline. Sci Rep. 2018;8:16972.

40. Mehta RL, Rabb H, Shaw AD, Singbartl K, Ronco C, McCullough PA, et al. Cardiorenal syndrome type 5: clinical presentation, pathophysiology and management strategies from the eleventh consensus conference of the acute dialysis quality initiative (ADQI). Contrib Nephrol. 2013;182:174–94.

41. Lekawanvijit S. Cardiotoxicity of uremic toxins: a driver of cardiorenal syndrome. Toxins (Basel). 2018;10:E352.

42. Russo D, Corrao S, Miranda I, Ruocco C, Manzi S, Elefante R, et al. Progression of coronary artery calcification in predialysis patients. Am J Nephrol. 2007;27:152–8.

43. Schwarz U, Buzello M, Ritz E, Stein G, Raabe G, Wiest G, et al. Morphology of coronary atherosclerotic lesions in patients with end-stage renal failure. Nephrol Dial Transplant. 2000;15:218–23.

44. Amann K. Media calcification and intima calcification are distinct entities in chronic kidney disease. Clin J Am Soc Nephrol. 2008;3: 1599–605.

45.•• Moody WE, Lin EL, Stoodley M, McNulty D, Thomson LE, Berman DS, et al. Prognostic utility of calcium scoring as an adjunct to stress myocardial perfusion scintigraphy in end-stage renal disease. Am J Cardiol. 2016;117:1387–96 **This study showed that coronary artery calcium score does not have an incremental value to myocardial perfusion imaging for prediction of adverse cardiac outcomes in renal transplant candidates.**

46. Wang LW, Fahim MA, Hayen A, Mitchell RL, Lord SW, Baines LA, et al. Cardiac testing for coronary artery disease in potential kidney transplant recipients: a systematic review of test accuracy studies. Am J Kidney Dis. 2011;57:476–87.

47. Herzog CA, Natwick T, Li S, Charytan DM. Comparative utilization and temporal trends in cardiac stress testing in U.S. medicare beneficiaries with and without chronic kidney disease. JACC Cardiovasc Imaging 2018 **[Epub ahead of print]**.

48. Gewirtz H, Dilsizian V. Integration of quantitative PET absolute myocardial blood flow in the clinical management of coronary artery disease. Circulation. 2016;133:2180–96.

49. Dilsizian V, Chandrashekhar Y, Narula J. Quantitative PET myocardial blood flow: trust, but verify. JACC Cardiovasc Imaging. 2017;10:609–10.

50. Schindler TH, Dilsizian V. PET-determined hyperemic myocardial blood flow: further progress to clinical application. J Am Coll Cardiol. 2014;64:1476–8.

51. Dilsizian V. Transition from SPECT to PET myocardial perfusion imaging: a desirable change in nuclear cardiology to approach perfection. J Nucl Cardiol. 2016;23:337–8.

52. Dilsizian V, Bacharach SL, Beanlands SR, Bergmann SR, Delbeke D, Dorbala S, et al. ASNC imaging guidelines/SNMMI procedure standard for positron emission tomography (PET) nuclear cardiology procedures. J Nucl Cardiol. 2016;23:1187–226.

53. Golzar Y, Doukky R. Stress SPECT myocardial perfusion imaging in end-stage renal disease. *Curr Cardiovasc Imaging Rep* 2017;10:Epub 2017 Mar 18.

54.•• Paz Y, Morgenstern R, Weinberg R, Chiles M, Bhatti N, Ali Z, et al. Relation of coronary flow reserve to other findings on positron emission tomography myocardial perfusion imaging and left heart catheterization in patients with end-stage renal disease being evaluated for kidney transplant. Am J Cardiol. 2017;120:1909–12 **This prospective study demonstrated for the first time that abnormal coronary flow reserve as assessed by positron emission tomography myocardial perfusion imaging is frequently present in patients with end-stage renal disease and is independent of perfusion defects or obstructive coronary artery disease.**

55. Fukushima K, Javadi MS, Higuchi T, Bravo PE, Chien D, Lautamäki R, et al. Impaired global myocardial flow dynamics despite normal left ventricular function and regional perfusion in chronic kidney disease: a quantitative analysis of clinical $^{82}$Rb PET/CT studies. J Nucl Med. 2012;53:887–8893.

56. Lodge MA, Braess H, Mahmood F, Suh JD, Englar N, Bacharach SL, et al. Developments in nuclear cardiology: transition from

single photon emission computed tomography to positron emission tomography-computed tomography. J Invasive Cardiol. 2005;17:491–6.

57. Dilsizian V, Taillefer R. Journey in evolution of nuclear cardiology: will there be another quantum leap with the F-18 labeled myocardial perfusion tracers? JACC Cardiovasc Imaging. 2012;5:1269–84.
58. Dilsizian V. Metabolic adaptation to myocardial ischemia: the role of fatty acid imaging. J Nucl Cardiol. 2007;14(Suppl 3):S97–9.
59. Tillisch J, Brunken R, Marshall R, Schwaiger M, Mandelkern M, Phelps M, et al. Reversibility of cardiac wall-motion abnormalities predicted by positron tomography. N Engl J Med. 1986;314:884–8.
60. Dilsizian V, Arrighi JA, Diodati JG, Quyyumi AA, Bacharach SL, Alavi K, et al. Myocardial viability in patients with chronic coronary artery disease: comparison of $^{99m}$Tc-sestamibi with thallium reinjection and $^{18}$F-fluorodeoxyglucose. Circulation. 1994;89:578–87.
61. Srinivasan G, Kitsiou AN, Bacharach SL, Bartlett ML, Miller-Davis C, Dilsizian V. $^{18}$F-fluorodeoxyglucose single photon emission computed tomography: can it replace PET and thallium SPECT for the assessment of myocardial viability? Circulation. 1998;97:843–50.
62. Kitsiou AN, Bacharach SL, Bartlett ML, Srinivasan G, Summers RM, Quyyumi AA, et al. 13N-ammonia myocardial blood flow and uptake: relation to functional outcome of asynergic regions after revascularization. J Am Coll Cardiol. 1999;33:678–86.
63. Osterholt M, Sen S, Dilsizian V, Taegtmeyer H. Targeted metabolic imaging to improve the management of heart disease. JACC Cardiovasc Imaging. 2012;5:214–26.
64.•• Sengupta PP, Kramer CM, Narula J, Dilsizian V. The potential of clinical phenotyping of heart failure with imaging biomarkers for guiding therapies: a focused update. *JACC Cardiovasc Imaging*. 2017;10:1056–71 **This review presents potential application of advanced cardiac imaging in assessment of heart failure phenotype and as a guide to selecting specific and evidence-based treatment.**
65. Gewirtz H, Dilsizian V. Myocardial viability: survival mechanisms and molecular imaging targets in acute and chronic ischemia. Circ Res. 2017;120:1197–212.
66.•• Fink JC, Lodge MA, Smith MF, Hinduja A, Brown J, Dinits-Pensy MY, et al. Pre-clinical myocardial metabolic alterations in chronic kidney disease. Cardiology. 2010;116:160–7 **This original prospective study showed for the first time that a significant inverse correlation existed between myocardial glucose utilization and severity of kidney dysfunction that could not be explained by demographic factors or cardiac workload.**
67. Amann K, Breitbach M, Ritz E, Mall G. Myocyte/capillary mismatch in the heart of uremic patients. J Am Soc Nephrol. 1998;9:1018–22.
68. McIntyre CW, Burton JO, Selby NM, Leccisotti L, Korsheed S, Baker CS, et al. Hemodialysis-induced cardiac dysfunction is associated with an acute reduction in global and segmental myocardial blood flow. Clin J Am Soc Nephrol. 2008;3:19–26.
69. Dasselaar JJ, Slart RH, Knip M, Pruim J, Tio RA, McIntyre CW, et al. Haemodialysis is associated with a pronounced fall in myocardial perfusion. Nephrol Dial Transplant. 2009;24:604–10.
70. Assa S, Hummel YM, Voors AA, Kuipers J, Westerhuis R, de Jong PE, et al. Hemodialysis-induced regional left ventricular systolic dysfunction: prevalence, patient and dialysis treatment-related factors, and prognostic significance. Clin J Am Soc Nephrol. 2012;7:1615–23.
71. Breidthardt T, Burton JO, Odudu A, Eldehni MT, Jefferies HJ, McIntyre CW. Troponin T for the detection of dialysis-induced myocardial stunning in hemodialysis patients. Clin J Am Soc Nephrol. 2012;7:1285–92.
72. Burton JO, Jefferies HJ, Selby NM, McIntyre CW. Hemodialysis-induced cardiac injury: determinants and associated outcomes. Clin J Am Soc Nephrol. 2009;4:914–20.
73. Dilsizian V, Bateman TM, Bergmann SR, Des Prez R, Magram M, Goodbody AE, et al. Metabolic imaging with β-methyl-ρ-[$^{123}$I]-iodophenyl-pentadecanoic acid (BMIPP) identifies ischemic memory following demand ischemia. Circulation. 2005;112(14):2169–74.
74. Taegtmeyer H, Dilsizian V. Imaging myocardial metabolism and ischemic memory. Nat Clin Pract Card. 2008;5:S42–8.
75. Dilsizian V. FDG uptake as a surrogate marker for antecedent ischemia. J Nucl Med. 2008;49:1909–11.
76. Dilsizian V, Fink JC. Deleterious effect of altered myocardial fatty acid metabolism in kidney disease. J Am Coll Cardiol. 2008;51:146–8.
77. Nishimura M, Hashimoto T, Kobayashi H, Fukuda T, Okino K, Yamamoto N, et al. Myocardial scintigraphy using a fatty acid analogue detects coronary artery disease in hemodialysis patients. Kidney Int. 2004;66:811–9.
78. Nishimura M, Murase M, Hashimoto T, Kobayashi H, Yamazaki S, Imai R, et al. Insulin resistance and impaired myocardial fatty acid metabolism in dialysis patients with normal coronary arteries. Kidney Int. 2006;69:553–9.
79. Nishimura M, Tsukamoto K, Hasebe N, Tamaki N, Kikuchi K, Ono T. Prediction of cardiac death in hemodialysis patients by myocardial fatty acid imaging. J Am Coll Cardiol. 2008;51:139–45.
80. Nishimura M, Tokoro T, Nishida M, Hashimoto T, Kobayashi H, Yamazaki S, et al. Myocardial fatty acid imaging identifies a group of hemodialysis patients at high risk for cardiac death after coronary revascularization. Kidney Int. 2008;74:513–20.
81. Moroi M, Tamaki N, Nishimura M, Haze K, Nishimura T, Kusano E, et al. Association between abnormal myocardial fatty acid metabolism and cardiac-derived death among patients undergoing hemodialysis: results from a cohort study in Japan. Am J Kidney Dis. 2013;61:466–75.
82. Nishimura M, Hashimoto T, Tamaki N, Kobayashi H, Ono T. Focal impairment in myocardial fatty acid imaging in the left anterior descending artery area, a strong predictor for cardiac death in hemodialysis patients without obstructive coronary artery disease. Eur J Nucl Med Mol Imaging. 2015;42:1612–21.
83. Eckelman WC, Dilsizian V. Chemistry and biology of radiotracers that target changes in sympathetic and parasympathetic nervous system in heart disease. J Nucl Med. 2015;56:7S–10S.
84. Schwartz PJ, De Ferrari GM. Sympathetic-parasympathetic interaction in health and disease: abnormalities and relevance in heart failure. Heart Fail Rev. 2011;16:101–7.
85. Kishi T. Heart failure as an autonomic nervous system dysfunction. J Cardiol. 2012;59:117–22.
86.•• Jacobson AF, Senior R, Cerqueira MD, Wong ND, Thomas GS, Lopez VA, et al. Myocardial iodine-123 meta-iodobenzylguanidine imaging and cardiac events in heart failure. Results of the prospective ADMIRE-HF (AdreView Myocardial Imaging for Risk Evaluation in Heart Failure) study. J Am Coll Cardiol. 2010;55:2212–21 **This is a pivotal study that lead to Federal Drug Administration's approval of meta-iodobenzylguanidine imaging for risk stratification of patients with heart failure and reduced systolic function.**
87. Dilsizian V, Chandrashekhar Y, Narula J. Introduction of new tests: low are the mountains, high the expectations. JACC Cardiovasc Imaging. 2010;3:117–9.
88.• Badarin FJ, Wimmer AP, Kennedy KF, Jacobson AF, Bateman TM. The utility of ADMIRE-HF risk score in predicting serious arrhythmic events in heart failure patients: Incremental prognostic benefit of cardiac $^{123}$I-mIBG scintigraphy. J Nucl Cardiol. 2014;21:756–62 **This was a post-hoc evaluation of data from**

**ADMIRE-HF that showed the utility of meta-iodobenzylguanidine imaging in predicting serious arrhythmic events in patients with heart failure and reduced systolic function.**

89. Agostini D, Belin A, Amar MH, Darlas Y, Hamon M, Grollier G, et al. Improvement of cardiac neuronal function after carvedilol treatment in dilated cardiomyopathy: a $^{123}$I-MIBG scintigraphic study. J Nucl Med. 2000;41:845–51.
90. Gerson MC, Craft LL, McGuire N, Suresh DP, Abraham WT, Wagoner LE. Carvedilol improves left ventricular function in heart failure patients with idiopathic dilated cardiomyopathy and a wide range of sympathetic nervous system function as measured by iodine 123 metaiodobenzylguanidine. J Nucl Cardiol. 2002;9:608–15.
91. Kasama S, Toyama T, Kumakura H, Takayama Y, Ichikawa S, Suzuki T, et al. Addition of valsartan to an angiotensin-converting enzyme inhibitor improves cardiac sympathetic nerve activity and left ventricular function in patients with congestive heart failure. J Nucl Med. 2003;44:884–90.
92. Kasama S, Toyama T, Kumakura H, Takayama Y, Ichikawa S, Suzuki T, et al. Spironolactone improves cardiac sympathetic nerve activity and symptoms in patients with congestive heart failure. J Nucl Med. 2002;43:1279–85.
93. Cha YM, Oh J, Miyazaki C, Hayes DL, Rea RF, Shen WK, et al. Cardiac resynchronization therapy upregulates cardiac autonomic control. J Cardiovasc Electrophysiol. 2008;19:1045–52.
94. Drakos SG, Athanasoulis T, Malliaras KG, Terrovitis JV, Diakos N, Koudoumas D, et al. Myocardial sympathetic innervation and long-term left ventricular mechanical unloading. JACC Cardiovasc Imaging. 2010;3:64–70.
95. Nishioka SA, Martinelli Filho M, Brandão SC, Giorgi MC, Vieira ML, Costa R, et al. Cardiac sympathetic activity pre and post resynchronization therapy evaluated by $^{123}$I-MIBG myocardial scintigraphy. J Nucl Cardiol. 2007;14:852–9.
96. Nakajima K, Verschure DO, Okuda K, Verberne HJ. Standardization of (123)I-meta-iodobenzylguanidine myocardial sympathetic activity imaging: phantom calibration and clinical applications. Clin Transl Imaging. 2017;5(3):255–63.
97. Kurata C, Wakabayashi Y, Shouda S, Okayama K, Yamamoto T, Ishikawa A, et al. Enhanced cardiac clearance of iodine-123-MIBG in chronic renal failure. J Nucl Med. 1995;36:2037–43.
98. Kurata C, Uehara A, Sugi T, Ishikawa A, Fujita K, Yonemura K, et al. Cardiac autonomic neuropathy in patients with chronic renal failure on hemodialysis. Nephron. 2000;84:312–9.
99. Chrapko BE, Jaroszyński AJ, Głowniak A, Bednarek-Skublewska A, Załuska W, Ksiażek A. Iodine-123 metaiodobenzylguanidine myocardial imaging in haemodialysed patients asymptomatic for coronary artery disease: a preliminary report. Nucl Med Commun. 2011;32:515–21.
100. Noordzij W, Özyilmaz A, Glaudemans AWJM, Tio RA, Goet ER, Franssen CFM, et al. Investigation into cardiac sympathetic innervation during the commencement of haemodialysis in patients with chronic kidney disease. Eur Radiol Exp. 2017;1:24.
101. Furuhashi T, Moroi M. Importance of renal function on prognostic value of cardiac iodine-123 metaiodobenzylguanidine scintigraphy. Ann Nucl Med. 2007;21:57–63.
102. Verschure DO, Somsen GA, van Eck-Smit BL, Verberne HJ. Renal function in relation to cardiac (123)I-MIBG scintigraphy in patients with chronic heart failure. Int J Mol Imaging. 2012;2012:434790.
103. Doi T, Nakata T, Hashimoto A, Yuda S, Wakabayashi T, Kouzu H, et al. Cardiac mortality assessment improved by evaluation of cardiac sympathetic nerve activity in combination with hemoglobin and kidney function in chronic heart failure patients. J Nucl Med. 2012;53:731–40.
104. Kouzu H, Doi T, Kawamukai M, Nishida J, Mochizuki A, Muranaka A, et al. Prognostic value of cardiac sympathetic imaging with metaiodobenzylguanidine for the prediction of mortality in patients with cardiorenal syndrome. Circulation. 2018;124:A9393.
105. Matsunari I, Aoki H, Nomura Y, Takeda N, Chen WP, Taki J, et al. Iodine-123 metaiodobenzylguanidine imaging and carbon-11 hydroxyephedrine positron emission tomography compared in patients with left ventricular dysfunction. Circ Cardiovasc Imaging. 2010;3:595–603.
106. Dilsizian V, Eckelman WC. Myocardial blood flow and innervation measures from a single scan: an appealing concept but a challenging paradigm. J Nucl Med. 2015 Nov;56(11):1645–6.
107. Castano A, Haq M, Narotsky DL, Goldsmith J, Weinberg RL, Morgenstern R, et al. Multicenter study of planar technetium 99m pyrophosphate cardiac imaging: predicting survival for patients with ATTR cardiac amyloidosis. JAMA Cardiol. 2016;1:880–9.
108. Chen W, Dilsizian V. Molecular imaging of amyloidosis: will the heart be the next target after the brain? Curr Cardiol Rep. 2012;14(2):226–33.
109. Chen W, Ton VK, Dilsizian V. Clinical phenotyping of transthyretin cardiac amyloidosis with bone seeking radiotracers in heart failure with preserved ejection fraction. Curr Cardiol Rep. 2018;20(4):23.
110. Pilebro B, Arvidsson S, Lindqvist P, Sundström T, Westermark P, Antoni G, et al. Positron emission tomography (PET) utilizing Pittsburgh compound B (PIB) for detection of amyloid heart deposits in hereditary transthyretin amyloidosis (ATTR). J *Nucl Cardiol*. 2018;25:240–8.
111. Pilebro B, Arvidsson S, Lindqvist P, Sundström T, Westermark P, Antoni G, et al. (123)I-Labelled metaiodobenzylguanidine for the evaluation of cardiac sympathetic denervation in early stage amyloidosis. Eur J Nucl Med Mol Imaging. 2012;39:1609–17.
112. Coutinho MC, Cortez-Dias N, Cantinho G, Conceição I, Oliveira A, Bordalo e Sá A, et al. Reduced myocardial 123-iodine metaiodobenzylguanidine uptake: a prognostic marker in familial amyloid polyneuropathy. Circ Cardiovasc Imaging. 2013;6(5):627–36.
113. Youssef G, Leung E, Mylonas I, Nery P, Williams K, Wisenberg G, et al. The use of 18F-FDG PET in the diagnosis of cardiac sarcoidosis: a systematic review and metaanalysis including the Ontario experience. J Nucl Med. 2012;53(2):241–8.
114. Blankstein R, Waller AH. Evaluation of known or suspected cardiac sarcoidosis. Circ Cardiovasc Imaging. 2016;9:e000867.
115. Tomberli B, Cecchi F, Sciagrà R, Berti V, Lisi F, Torricelli F, et al. Coronary microvascular dysfunction is an early feature of cardiac involvement in patients with Anderson-Fabry disease. Eur J Heart Fail. 2013;15:1363–73.

**Publisher's Note** Springer Nature remains neutral with regard to jurisdictional claims in published maps and institutional affiliations.